High-resolution study of $^1P^o$ double-excitation states in helium

M. Domke, K. Schulz, G. Remmers, and G. Kaindl
Institut für Experimentalphysik, Freie Universität Berlin, Arnimallee 14, D-14195 Berlin-Dahlem, Germany

D. Wintgen*
Fakultät für Physik, Universität Freiburg, Hermann-Herder-Strasse 3, D-79104 Freiburg, Germany
(Received 31 March 1995; revised manuscript received 21 August 1995)

We describe extensive results on the $^1P^o$ double-excitation resonances of He below the $N=2$–9 ionization thresholds obtained recently by high-resolution photoionization measurements using synchrotron radiation from the SX700/II monochromator at the Berliner Elektronenspeicherring für Synchrotronstrahlung (BESSY). The resonance energies, linewidths, Fano-q parameters, and quantum defects of the various Rydberg resonances, derived from the experimental data, are compared in detail with the results of *ab initio* calculations employing the complex-rotation method. All three optically allowed Rydberg series below the $N=2$ ionization threshold were identified. For $3 \leqslant N \leqslant 8$, the two most intense Rydberg series were resolved below each threshold, and for $N=3$, one state of a third series could be identified. For the higher Rydberg series ($N \geqslant 5$), the two neighboring series, N and $N+1$, generally interfere, which has a strong influence on the transition intensities, linewidths, and quantum defects of the principal series. All together, states of 18 different Rydberg series in the $^1P^o$ double-excitation resonance region of He were observed.

PACS number(s): 32.80.Dz, 32.70.Jz, 31.25.Jf

I. INTRODUCTION

Doubly excited helium is often considered to be the prototype of atomic systems with electron correlation, since—due to its simplicity—it is also accessible to rigorous theoretical treatments. Nevertheless, most of the details of doubly excited He remained unexplored until a few years ago, even though the first experimental and theoretical results on double-excitation resonances in He had been obtained more than 30 years ago [1,2]. It then became clear that the two excited electrons are strongly correlated and can no longer be characterized as $s,p,d,f,...$ electrons; instead, new quantum numbers taking correlation into account had to be introduced.

The electronic excitations to the first double-excitation $^1P^o$ Rydberg series, with the ''inner'' electron in the $N=2$ shell and the ''outer'' electron in the $n=2,3,4,...$ shells, cover the energy region from 60 to 65.4 eV, i.e., from the lowest $^1P^o$ double-excitation state ($N=2$, $n=2$) up to the $N=2$ ionization threshold of He, I_2, which is the $N=2$ state of He^+. With the inner electron excited to higher quantum numbers, the $N=3,4,5,...$ double-excitation Rydberg series are obtained, extending up to the double-ionization threshold, $I_\infty \cong 79$ eV. Until 1990, reliable experimental results on the double-excitation resonances in He were confined to the $N=2$ Rydberg series [1,3,4] as well as to the first members of higher Rydberg series with relatively short natural lifetimes [4–7]. Two Rydberg series converging to I_2 were known, which had been resolved at that time up to the $n=10$ and $n=5$ resonances, respectively [1]. Resonances of the $N=3$, 4, and 5 Rydberg series had been identified up to $n=8$ [1,6,7]. Accurate line-shape analyses were only available for the lowest resonances, namely, the ($N=2$, $n=2$) and ($N=3$, $n=3$) states [4–7].

In the past few years, a renewed interest in the study of such excitations emerged, reflected in the publication of the results of several *theoretical* studies. Until quite recently, however, the experimental data lagged considerably behind the theoretical progress, mainly due to the lack of suitable monochromatic photon sources for high-resolution spectroscopic studies in this energy region. This problem has been overcome by the development of high-resolution monochromators at synchrotron-radiation facilities. In the energy range of interest, the most successful beamline in the past five years had been the SX700/II monochromator, operated by the Freie Universität Berlin at the Berliner Elektronenspeicherring für Synchrotronstrahlung (BESSY) [8].

The photoionization studies performed on He atoms in the ground state limit the final states to $^1P^o$ symmetry due to the dipole selection rules. This limitation, on the other hand, facilitates the assignment of the double-excitation resonances of He observed in the energy region from 60 to 79 eV, with overlapping Rydberg series and interseries interferences. Four years ago, these Rydberg series could be investigated with the SX700/II beamline up to $N=6$, providing a substantially improved data set on the most intense series [9]. More recently, however, both the resolution and the photon flux available at the SX700/II monochromator were further improved, allowing each series to be followed up to higher quantum numbers n, and additional Rydberg series were found for the first time. These improvements resulted in the observation of the third Rydberg series below I_2 [10], which had been ''hidden'' up to then, and of at least one additional secondary series for each quantum number N [11]. These experimental results stimulated again further theoretical work on double-excitation resonances in He [12–16].

The present paper describes the status of our experimental work on double-excitation resonances in He. It reviews the

*Deceased.

previously published recent experimental results [9–11] and describes in addition a number of new results. As examples, all of the principal Rydberg series could be resolved now to much higher quantum numbers n than before, and several Rydberg series were observed for the first time, including those below I_7, I_8, and I_9, as well as the relatively weak (secondary) Rydberg series accompanying all of the most intense (principal) series [11]. In addition, the energies, linewidths, Fano-q parameters, and oscillator strengths obtained from the experimental data are compared in detail with the results of *ab initio* calculations based on the complex-rotation method. Both the experimental and the theoretical results are compared with the results of other previous publications.

II. EXPERIMENTAL PROCEDURES

The measurements were performed with the SX700/II monochromator at BESSY operated by the Freie Universität, Berlin [8], which is equipped with a plane premirror, a plane grating, an ellipsoidal focusing mirror, and an exit slit. The monochromator has no entrance slit, and thus position and size of the electron beam source influence strongly both energy calibration and resolution. An improvement in resolution can be obtained by using a grating with a high density of lines as well as an electron beam with a small size and high stability. In the present work, we used a 2442-line/mm grating, and BESSY was operated in the small-source mode, where the vertical beam size was reduced to $\cong$0.12 mm. The best energy resolution was achieved in the photon energy range of interest when only $\cong$20% of the full area of the ellipsoidal mirror were illuminated. This optimum in the shaded-off mirror area resulted from a tradeoff between two effects that improve and deteriorate, respectively, spectral resolution: A shaded-off mirror first improves resolution by diminishing the figure error of the ellipsoidal mirror from a value of $\cong$0.65 arcsec, typical for the full mirror, to a value of $\cong$0.40 arcsec for the shaded-off mirror; on the other hand, it deteriorates resolution by diffraction at the confining diaphragms [8]. It should be mentioned here that progress in small-source optics at BESSY allows us to now operate this electron storage ring in the small-source mode with beam currents exceeding 500 mA, causing only a moderate decrease in beam lifetime (by a factor of $\cong$2) as compared to normal-source optics.

The resolution of the monochromator was determined by studying long-lived double-excitation resonances of He with very small natural linewidths, in particular some double excitations below I_2. This resulted in $\Delta E \cong 4$ meV [full width at half maximum (FWHM)] at $h\nu = 64$ eV, corresponding to a resolving power of $E/\Delta E \cong 16\,000$ [10]. Note that the resolution ΔE scales with $E^{3/2}$ for this type of monochromator. The photon energy was calibrated by the $C1s^{-1}\pi^*$, $v'=0$ resonance in the inner-shell excitation spectrum of CO in the gas phase at 287.40 eV [17] as well as by the He double-excitation resonance $2,1_3$ $(sp,23-)$ at 62.7580 eV [10,16]. Energy calibration was a crucial point in the present measurements, since any instability in source position or monochromator adjustment would shift the energy scale: Thus frequent calibration measurements were performed.

The double-excitation resonances were observed via their decay by autoionization and by monitoring the total photoionization current in the 10^{-12}-A range as a function of photon energy. These photoionization measurements were performed with a two-plate ionization cell of 10-cm active length [8], filled with He at a pressure in the range of 0.01–3 mbar, and separated from the UHV of the monochromator by a 1200-Å-thick carbon window. A voltage of 100 V was applied between the two plates to collect the electrons and ions, and the current was measured with a sensitive ammeter (Keithley, model 617). For the $N=2$ Rydberg series ($h\nu = 60$–65.4 eV), as well as for the lower $N=3$ series ($h\nu = 70$–72.5 eV), higher photon transmission and therefore an improved signal-to-noise ratio was achieved using a 1500-Å-thick Al (1% Si) window. This window material, however, could not be employed for photon energies exceeding 72.5 eV due to strong absorption and modulations of the transmitted photon flux above the Al $L_{2,3}$ absorption thresholds.

In each experiment, the He pressure was chosen as high as tolerable without inducing noticeable saturation effects that would influence line shapes, intensities, and linewidths. Nevertheless, signal saturation must be carefully considered, both in case of intense resonances and also for weak resonances sitting on a high background. The photon beam entering the gas cell, J_0, is weakened by photoabsorption (cross section σ) throughout the gas cell with a gas density ρ and a plate length L according to the Lambert-Beer law. Assuming a constant electron-ion yield per photoabsorption event, one arrives at an ionization current of $J = J_0 e^{-\rho\sigma l_d}(1-e^{-\rho\sigma L})$; here, l_d is the length of the ''dead volume'' in front of the plates, where photons are absorbed *without* contributing to the ionization current. For an unsaturated spectrum with $\rho\sigma L \ll 1$, we obtain $J = J_0 \cdot \rho\sigma L$, and the measured current is proportional to the absorption cross section. For higher pressures, saturation effects set in, first in a moderate way by broadening the absorption line, since the beam intensity is predominantly weakened at the energies of the most intense spectral lines, in particular at the maxima of the resonance lines. For higher pressures, this effect may even result in an apparent splitting of lines and/or a reversion of the line profiles. As a consequence, a Lorentzian line can even change by these saturation effects to an apparent ''window'' resonance, with negative absorption relative to background.

III. CLASSIFICATION OF DOUBLE-EXCITATION STATES IN He

Various classification schemes for the double-excitation states in He are in use. This is a consequence of the different theoretical approaches used to describe strong correlation between the two electrons in He. Due to the optical absorption method, the resonances observed in the present work are restricted by the dipole selection rules to $^1P^o$ final states. For each N, a total of $(2N-1)$ $^1P^o$ Rydberg series are predicted by theory, converging to the same ionization threshold of He, I_N, with the inner electron in the Nth quantum state of He^+.

All classification schemes use N for the main quantum number of the inner electron and n for the outer electron. The ''old'' classification scheme by Madden and Codling [1] is the simplest one, but it is only well suited for the three Rydberg series converging to I_2. In this scheme, the three $N=2$ $^1P^o$ Rydberg series are denoted by $(sp,2n+)$,

$(sp,2n-)$, and $(2p,nd)$, where $(sp,2n+)$ and $(sp,2n-)$ stand for the addition and subtraction, respectively, of the wave functions $\psi(2p,ns)$ and $\psi(2s,np)$. In a second rather simple classification scheme, the series is just marked by $a,b,c,...$ in the order of decreasing oscillator strengths. A later introduced scheme is based on an analogy between the "three-body" double-excitation states in He and molecular states [18].

The classification scheme most widely used is based on a hyperspherical coordinate description of He introduced by Herrick and Sinanoglu [19] and Lin [20], where new correlation quantum numbers T (with $T=0$ or 1), K [ranging from $N-1-T$, $N-3-T$,... to $-(N-1-T)$], and A (with $A=+1$, -1, 0; abbreviated by "+,""−,"0) were introduced describing the angular (T,K) and radial (A) correlations. In this scheme, the double-excitation states are denoted by $n(K,T)^A_N$. There are $(N-1)$ series with $T=1$ and $A=$"+" $(N-1)$ series with $T=0$ and $A=$"−," and only one series with $T=0$ and $A=$"0" for each N value. The most intense series observed in photoabsorption have $T=1$ and $A=$"+," and nearly all excited resonances fulfill this approximate "selection rule" (for exceptions, see below). Among these, the leading series with the highest oscillator strength is always given by $K=N-2$. It has been shown that a two-electron atom can be described in analogy to a three-atom linear molecule, giving the angular quantum numbers of the two-electron atom a physical meaning as bending vibrations, with the vibrational quantum number $v=(N-K-T-1)/2$ [21]. Along this line, Rydberg series with the same v values are said to have the same symmetry.

In Lin's classification scheme, the ground state of He is $1(0,0)^+_1\ {}^1S^e$. The complete set of the three $^1P^o$ double-excitation series below I_2, denoted in the "old" classification scheme by $(sp,2n+)$, $(sp,2n-)$, and $(2p,nd)$, is given in Lin's classification by $n(0,1)^+_2$, $n(1,0)^-_2$, and $n(-1,0)^0_2$ [20]. Only the first of these series, the principal one, fits into the common $T=1$, $A=$"+" relation, while the two other $N=2$ series do not. Below I_3, five $^1P^o$ series can be photoexcited from the ground state of He, namely, $n(1,1)^+_3$, $n(-1,1)^+_3$, $n(2,0)^-_3$, $n(0,0)^-_3$, and $n(-2,0)^0_3$, with only two of them fulfilling the $T=1$, $A=$"+" relation. In the present work, Lin's classification scheme is used in an abbreviated form, N,K_n, as introduced by Zubek *et al.* [7]. This is done for *all* Rydberg series, i.e., the $T=1$ series are written as $N,(N-2)_n$, $N,(N-4)_n$, $N,(N-6)_n$,..., the $T=0$ series as $N,(N-1)_n$, $N,(N-3)_n$,... . For $N=2$, the $T=1$ series is $2,0_n$, and the two $T=0$ series are $2,1_n$ and $2,-1_n$, instead of the old notations $(sp,2n+)$, $(sp,2n-)$, and $(2p,nd)$, respectively. Similarly, the $N=3$ series are written as $3,1_n$ and $3,-1_n$ for $T=1$ as well as $3,2_n$, $3,0_n$, and $3,-2_n$ for $T=0$; the $N=4$ series are $4,2_n$, $4,0_n$,..., and so on.

IV. THEORETICAL DESCRIPTION

The theory of autoionization goes back to the year 1961, when Fano described photoabsorption in the vicinity of an autoionizing resonance, which coincides in energy with a continuum [22]. In case of double excitation in He, the Rydberg series converging to the $N=2$ threshold interact with the continuum above the $N=1$ ionization threshold of He, I_1; the $N=3$ Rydberg series may interact with the continua above I_1 and I_2, etc. (see Fig. 1). The typical Fano profile consists of a constructive and a destructive interaction of the direct photoionization channel with the photoionization channel via double excitation. This results in the well-known Fano profile of the cross section,

$$\sigma(E)=\sigma_a\,\frac{(q+\varepsilon)^2}{1+\varepsilon^2}+\sigma_b,\quad \text{with}\quad \varepsilon=2\,\frac{E-E_r}{\Gamma},\qquad (1)$$

where E_r is the resonance energy, Γ is the linewidth (FWHM), and q^2 represents the ratio of the transition probabilities to a discrete state and to the continuum ("Fano-q parameter") [22]. The profile index q can vary from $|q|\to\infty$, when the transition probability into the discrete state is dominant (Lorentzian profile), to $q\to 0$, when the transition probability into the discrete state is much smaller than that into the continuum, leading to a symmetric decrease of the cross section to a minimum value ("window" resonance). According to Fano and Cooper [23], the Fano-q parameter is approximately constant within a given Rydberg series, and the linewidths, Γ_n, and transition probabilities, P_n, of the individual resonances of a given Rydberg series decrease according to the third power of the reduced quantum number $n^*=n-\delta$ (δ is the quantum defect), leading to a constant reduced linewidth, $\Gamma^*=\Gamma_n\ n^{*3}$ and to a constant reduced transition probability, $P^*=P_n\ n^{*3}$. In the case of many resonances interacting with each other and with various continua, the cross section can be represented by a sum of single Fano profiles.

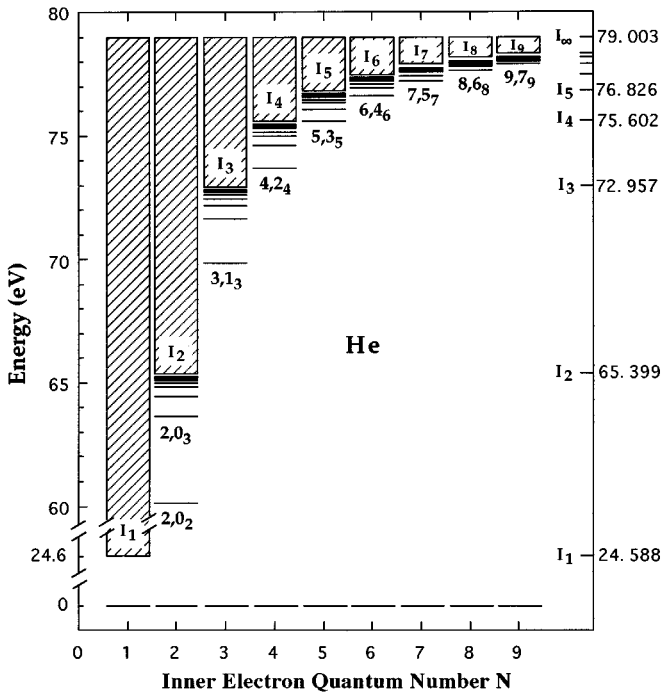

FIG. 1. Term scheme of $^1P^o$ double-excitation resonances in He with energies taken from the present complex-rotation-method calculations. Only the principal series, $N,(N-2)_n$, converging to the He (N) thresholds, I_N, are shown. Above I_N, a He^+ ion in quantum number N and a free electron are left behind (hatched regions); I_N converges to the I_∞ threshold in a hydrogenic way. Note the energy overlap of neighboring series for $N>4$.

The observed Fano profiles originate typically from an interaction of the discrete double-excitation states with the *nearby* continuum, i.e., the N,K_n series interacts predominantly with the $(N-1)$ continuum. Rydberg series with equal N values, but with different correlation quantum numbers K, will normally differ in their q values due to the special discrete states involved as well as the different parts of the continuum they interact with. For higher N, additional channels for interaction are opened: Overlaps of neighboring Rydberg series occur for $N \geqslant 5$, when the first member of the Nth series overlaps in energy with the higher members of the $(N-1)$th series (see Fig. 1), leading to interseries interferences. In this case, strong variations of the reduced transition probability as well as of the reduced linewidth within a given Rydberg series are theoretically expected.

A. Recent theoretical approaches

To calculate the double-excitation resonances in He, both in the undisturbed and the interfering-series region, various theoretical approaches are in use. One frequently followed procedure of describing electron correlation in the double-excitation region is based on the multichannel quantum defect theory (MQDT), which is a phenomenological theory somewhere in between an independent-electron picture and many-electron theories. MQDT handles interseries interferences as a three-channel problem, with one closed channel N, one open channel $(N-2)$, and one further channel $(N-1)$ that is open above I_{N-1} and closed below it. Applied to the $5,3_n$ series of He, this means that the $6,4_6$ resonance (closed channel) interacts with the $5,3_n$ resonances (partially closed channel) and the $N=4$ continuum (open channel). As shown recently [9], this approximation provides a rather good description of interseries interferences.

A substantial set of calculations of double excitations in He exists [24–64]; most of the early work below the $N=2$ [24–28,36–38] and $N=3$ thresholds [29–35] has been compiled in previous experimental work [3,5,6]. In the past decade, more than 30 new theoretical papers on double-excitation states in He have appeared in the literature. The various approaches include the pseudostate close-coupling method [46], the Feshbach method with saddle-point technique [47], the L^2 technique [48–51,59,62], the R-matrix method [43,55], the diabatic and adiabatic hyperspherical

TABLE I. Summary of results obtained with the complex-rotation-method calculations for the $^1P^o$ double-excitation Rydberg series: Reduced transition probability, P^*, quantum defect, δ, reduced linewidth, Γ^*, and absolute linewidth of the lowest reonance in each Rydberg series, $\Gamma_{n=N}$. The quantum defects and the reduced quantities are restricted to $n \geqslant N+2$ as well as to noninterfering regions in each series. P^* values are given in % of the reduced transition probability of the most intense series, $2,0_n$ ($\equiv 100$); series with $P^* < 0.01$ (marked by $\cdots$) are omitted. A dash means that the respective series does not exist; linewidths are given in meV.

	$N=2$	$N=3$	$N=4$	$N=5$	$N=6$	$N=7$
$N,(N-2)_n$						
P^*	100	20	7	3	1	$\cong 0.5$
$\delta_{n>N+1}$	0.18	0.84	1.4	2.0	2.3	$\cong 2.7$
Γ^*	200	3100	3000	3300	3200	$\cong 3500$
$\Gamma_{n=N}$	37	190	97	60	40	30
$N,(N-4)_n$						
P^*	–	2	0.7	0.56	0.3	0.08
δ		-0.2	0.7	1.3	1.8	$\cong 2.3$
Γ^*		600	6300	6000	6500	$\cong 6900$
$\Gamma_{n=N}$		40	130	89	68	65
$N,(N-6)_n$						
P^*	–	–	0.06	0.02	$\cdots$	$\cdots$
δ			-0.6	0.5		
Γ^*			1000	3800		
$\Gamma_{n=N}$			21	50		
$\cdots$	–	–	–	$\cdots$	$\cdots$	$\cdots$
$N,(N-1)_n$						
P^*	1.7	0.02	$\cdots$	$\cdots$	$\cdots$	$\cdots$
δ	0.72	1.3				
Γ^*	2.0	0.01				
$\Gamma_{n=N}$	0.1	0.9				
$N,(N-3)_n$						
P^*	0.35	$\cdots$	$\cdots$	$\cdots$	$\cdots$	$\cdots$
δ	-0.25					
Γ^*	0.01					
$\Gamma_{n=N}$	0.0003					
$\cdots$	–	$\cdots$	$\cdots$	$\cdots$	$\cdots$	$\cdots$

TABLE II. Results for the $5,3_n$ ($6,4_n$) series interfering with the $6,4_6$ ($7,5_7$) intruder state, as obtained from complex-rotation-method calculations, resulting in anomalies in quantum defects, δ_n, reduced linewidths, Γ_n^*, reduced transition probabilities, P_n^*, and Fano-q_n parameters. Linewidths are given in meV. δ_n, Γ_n, and q_n values are compared to hyperspherical close-coupling calculations [15], using the hydrogenic values I_5=0.08 a.u.=76.8264 eV and I_6=0.05556 a.u.=77.4914 eV.

	This work					Ref. [15]		
n	δ_n	Γ_n	Γ_n^*	q_n	P_n^*	δ_n	Γ_n	q_n
				$5,3_n$				
5	1.718	59.3	2100	−0.207	1.47	1.717	61.5	
6	1.721	42.5	3330	−0.022	2.97	1.728	41.1	−0.027
7	1.819	25.2	3500	−0.006	3.25	1.824	25.2	−0.012
8	1.903	12.4	2800	0.006	2.60	1.914	12.7	−0.014
9	2.011	3.0	1030	0.067	0.88	2.023	3.9	
10	2.327	3.5	1580	0.538	1.65	2.335	3.5	
11	2.727	11.9	7750	0.190	7.64	2.730	12.4	
12	2.870	7.9	6010	0.046	6.72	2.871	8.5	
13	2.919	5.0	5120	0.02	5.60	2.878	5.3	
14	2.947	3.4	4590			2.777	3.7	
15	2.966	2.6	4530					
				$6,4_n$				
6	2.111	40.6	2390			2.110	40.5	
7	2.133	32.3	3720	−0.45	1.60	2.130	31.3	
8	2.266	19.5	3680	−0.42	1.64	2.273	19.6	
9	2.411	5.7	1740	−0.33	0.68	2.425	6.1	
10	2.834	5.2	1910	−0.03	0.98	2.793	5.0	
11	3.281	14.0	6440	−0.29	3.55	3.287	12.9	
12	3.412	8.9	5640	−0.02	4.48	3.428	8.3	
13	3.463	4.5	3900	−0.4	1.84	3.461	4.4	
14	3.506	2.7	3120			3.346	3.1	
15	3.544	1.5	2260			3.256	1.3	
16	3.583	0.8						

method [45,52], the hyperspherical close-coupling method [13–15], and the method of complex rotation [16,34,35,39,53,54,61,64]. Resonance energies, linewidths, and to some extent also Fano-q parameters have been calculated for the $^1P^o$ double-excitation resonances in He below the $N=2$ threshold [12,14,16,39–53], below the $N=3$ threshold [16,47,52,54–61], below the $N=4$ threshold [16,52,54,55,62,63], and for $N\geqslant 5$ [13,15,54]. Since the present paper deals predominantly with new experimental results, no critical evaluation of the various theoretical methods is given here.

The method of complex rotation [65,66], however, is used here for calculating resonance energies, linewidths, and Fano-q parameters in order to allow a detailed comparison with the experimental results. In this method, the many-electron Hamiltonian is transformed into complex coordinates, and ''hidden'' resonances are ''exposed'' by an appropriate rotation of the energy scale of unbound states beyond the thresholds, I_N. The wave functions are transformed to perimetric coordinates and are expanded in a Sturmian-type basis set [16]. The convergence is checked by systematically increasing the set of basis functions including up to 48 shells for the interfering series. As a consequence, the natural linewidths result directly from the imaginary part of the energy eigenvalues, and the Fano-q parameters are obtained from the dipole-transition matrix elements d from the ground state, $q=-\mathrm{Re}(d)/\mathrm{Im}(d)$ [16]. The cross section can be written as a sum of simple Fano profiles in Eq. (1) [67].

The complex-rotation method provides also good results for interseries interferences (see below). Up to now, the results of only very few calculations of interseries interferences in He have been published: Apart from MQDT adaptions of experimental data [9], only fairly recent hyperspherical close-coupling calculation of such interferences are known [13,15]. The variations of the excitation cross section resulting from the most recent calculation [15] agree quite well with the present theoretical and experimental results [9]. It should also be noted that the authors in Ref. [13] use a peak assignment that differs from the one used here: in Ref. [13], e.g., the $6,4_6$ resonance, which is the perturber of the $5,3_n$ series, emerges individually, whereas in the present paper, the $6,4_6$ perturber is taken to vanish behind the long-lived $5,3_n$ resonances. The present assignment seems to be more suitable, since it includes a smooth variation of the quantum defect as a function of n within a given series, with a *gradual* increase by one in the interference regions (see below, chapter 6).

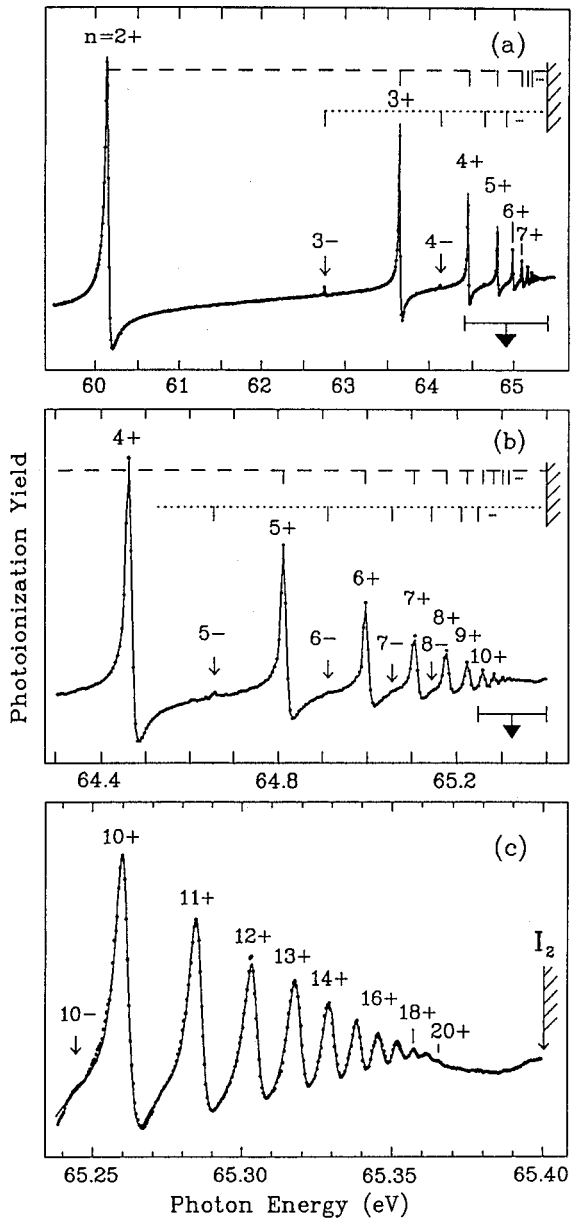

FIG. 2. Autoionizing resonances of doubly excited He below the $N=2$ threshold (I_2) of He; from Ref. [10]: (a) overview; (b) 5.3 times expanded view of the $n\geqslant 4+$ region; (c) 36 times expanded view of the $n\geqslant 10+$ region. The principal $2,0_n$ series is denoted by $n+$, the secondary series $2,1_n$ by $n-$. In (a) and (b), the "+" and "−" $^1P^o$ series are indicated by vertical bar diagrams and dashed and dotted lines, respectively.

B. Results of complex-rotation-method calculations

In the following, the properties of the various Rydberg series are discussed, as obtained by calculations based on the complex-rotation method. In Table I, transition probabilities, P, quantum defects, δ, and linewidths, Γ, are given. For each series, typical *reduced* transition probabilities, P^*, and reduced linewidths, Γ^*, are listed. The reduced values as well as the quantum defects are approximately constant within a given Rydberg series. For the linewidths, Γ_n, also absolute values are listed for each first resonance ($n=N$) in a given series.

There are, however, some deviations from constant P^*, Γ^*, and δ values within a given series: (i) For $n=N$ ("Wannier-ridge" state), the excited electrons interact more strongly, causing a slight increase in the quantum defect and a lowering of the resonance energy of the N,K_N state by $\cong$150 meV as compared to the $n>N$ resonances. (ii) There is a rather small increase of $\delta(n)$ as a function of n within all principal series with $N>2$ (not shown in Table I, see below). This increase is stronger for high-N series and may be caused by the polarizability of the doubly excited He atom. This effect depends additionally on the angle θ_{12} between the coordinates of the two electrons and is strongest for $\theta_{12}\cong 180°$. For the $2,0_n$ series ($\theta_{12}=90°$), there is even a decrease of $\delta(n)$ with increasing n. (iii) Most strikingly, there is a strong variation in P^*, Γ^*, and δ for interfering Rydberg series, as is demonstrated in Table II. For high-N series ($N\geqslant 5$), the lowest resonance ($n=N$) overlaps in energy with the high-n members of the $(N-1)$th neighboring series, causing the series to perturb each other. As a consequence of this interference, the short-lived N,K_N resonances are "eaten up" by the long-lived $(N-1),K_n$ resonance at the same energy, and δ, Γ^*, and P^* are changing accordingly. A typical interference pattern is shown in Table II for the $5,3_n$ and the $6,4_n$ series: both the reduced transition probability and the reduced linewidth as a function of quantum number n follow a Fano-like profile, with minima and maxima in P_n^* and Γ_n^*, and the quantum defect increases by one in the interference region. In these cases, the n dependence of P^* and Γ^* is represented by an index n, P_n^* and Γ_n^*. It should be noted that the results of both the hyperspherical close-coupling calculations [15] and the present complex-rotation calculations for the $5,3_n$ and the $6,4_n$ series are in excellent agreement.

The P^* values given in Table I enable one to perform a *crude* estimate of the intensities of the various series, allowing a judgement whether a series ought to be visible or not in a photoionization experiment. We see that for the principal series, $N,(N-2)_n$, the P^* values diminish by factors of 2 to 3 when going from N to $N+1$, and only the $N=2$ series is more intense (by a factor of $\cong$5 relative to the $N=3$ series). For secondary series, $N,(N-4)_n$, P^* diminishes by factors of $\cong$10 relative to the principal series. P^* values of the $T=0$ series, $N,(N-1)_n$, $N,(N-3)_n$,... amount to only 1–2% of those of the $T=1$ series, $N,(N-2)_n$, $N,(N-4)_n$,... .

V. EXPERIMENTAL RESULTS

A. Data-fitting procedure

All spectra discussed in this work were least-squares fitted by superpositions of Fano line shapes convoluted with the monochromator function. From fits of the $2,1_n$ and $2,-1_n$ resonance lines, with linewidths much narrower than the present instrumental resolution, it turns out that the monochromator function is not a pure Gaussian, but contains also a non-Gaussian contribution that can be approximately described by a Lorentzian shape. A detailed analysis shows that the monochromator function, ΔE, is well described by $\cong$60% Gaussian and $\cong$40% Lorentzian contributions. Such a detailed analysis of the monochromator function was only possible due to the considerably improved signal-to-noise ratio in the present data. Previously, fairly good fits of the He double-excitation spectra had been achieved with a pure

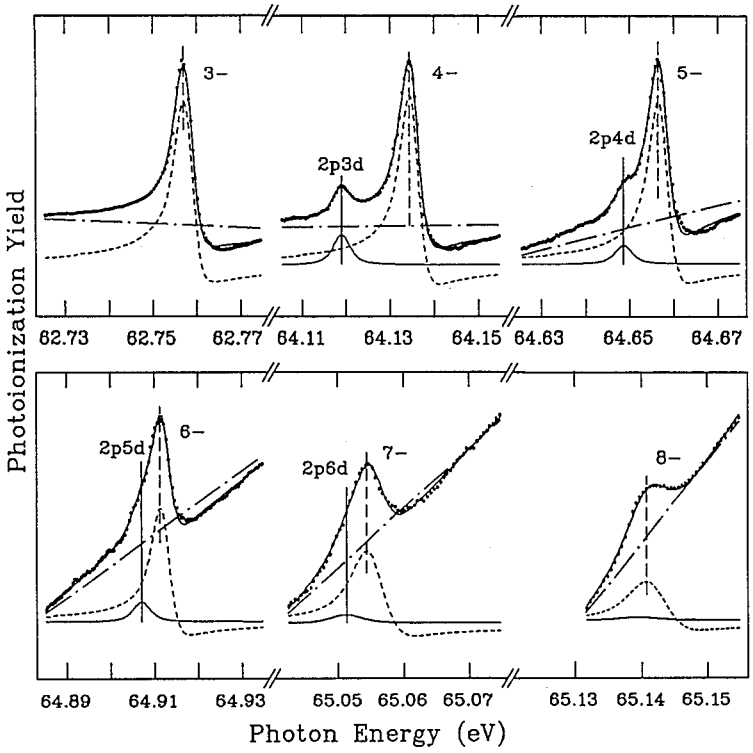

FIG. 3. $2,1_n$ and $2,-1_n$ $^1P^o$ resonances of doubly excited He; from Ref. [10]. The resonances of the $2,1_n$ series are again denoted by $n-$, while those of the $2,-1_n$ series are marked by $2pnd$. For higher n values, the resonances sit on increasingly steep slanting backgrounds caused by the leading edges of the neighboring $2,0_n$ states ($n+$ states in Fig. 2), which are out of scale in this figure.

Gaussian monochromator function [9]. It is remarkable that the relative weights of the Gaussian and Lorentzian contributions to the monochromator function are very similar to those observed with the SX700/II monochromator at higher photon energies, e.g., at the $N1s\rightarrow\pi^*$ excitation of the N_2 molecule at $h\nu\cong 401$ eV [8].

After removing an approximately linear background from the raw data, caused mostly by the decay of the electron current in the BESSY storage ring, positions and linewidths of the resonance lines were determined as follows: In a first approximation, the resonances belonging to a particular series, excluding the first members, were assumed to fit the Rydberg formula with constant quantum defect, δ. With the ionization threshold obtained in this way, exact δ values were then determined for each resonance line. The reduced linewidths, Γ^*, of the individual resonances in a given series were assumed to be constant, again excluding the first two or three members. For the high-n members of a series, the linewidths decrease rapidly to values far below experimental resolution. Note that constant Γ^*, P^*, and q values mean constant peak heights of the Fano profiles of the resonance lines (peak excitation cross sections). In order to correctly convolute these extremely narrow intrinsic Fano profiles of the high-n resonances with the monochromator function, the point density had to be artificially increased to $\cong$100 points per meV. This resulted in a correct description of the observed decrease in the intensities of the high-n resonance lines. However, it also led to substantial increases in computation time [8].

Obviously, the described fit procedures can only be applied to Rydberg series *without* interseries interferences, i.e., for $N\leqslant 4$. No restrictions on line positions and linewidths were applied for resonances with $N\geqslant 5$ with interseries interferences. In the interference regions, the thresholds I_N for $N\geqslant 5$ were obtained by using the thresholds I_N for $N=1$–4, the double-ionization threshold $I_\infty=79.003$ eV, and the Rydberg formula $I_N=I_\infty-4R_{\rm He}/N^2$, with $R_{\rm He}=13.60383$ eV [50]. This method is based on the assumption that the I_N values converge towards I_∞ in a hydrogenic way.

B. Resonances below the $N=2$ threshold

In Figs. 2 and 3, the photoionization spectra of He below I_2 ($h\nu=65.402$ eV) are shown. Besides the dominant resonances of the principal "+" series, $(2,0_n)$, weak "−" resonances of the secondary series, $(2,1_n)$, are observed at lower energies than the respective members of the "+" series; both series converge towards the same ionization threshold, I_2. These series have been resolved up to the $n=20$ and $n=11$ states for the "+" and "−" series, respectively. The resonance lines exhibit Fano profiles due to interaction of the discrete double-excitation states with the continuum; for the "+" and "−" series, respectively, $q=-2.5$ and -3.2 were obtained.

Figure 2 shows that the peak heights of the "+" resonances decrease steadily with increasing n. This is just a consequence of the convolution of the approximately constant monochromator function with the intrinsic Fano profiles of the resonances with rapidly decreasing linewidths. In this way, the peak heights of the observed resonances are measures for both the linewidths and the monochromator function. Simulations show that the number n_m of resolved

TABLE III. Comparison between experimental and theoretical values for resonance energies, E_n, linewidths (FWHM), Γ_n, and Fano-q parameters of the first members of the $N=2$ double-excitation Rydberg series of He. Unless otherwise stated, the error bars of the experimental values are ± 1 in the last digit. Note that the *relative* energies are given with an accuracy of ± 1 meV, but the *absolute* energies both in experiment and in theory are uncertain to ± 4 meV. This is due to minor changes in monochromator calibration as well as to a scattering of values assumed for the double-ionization threshold, I_∞, ranging from 79.003 to 79.008 eV. Literature values given in a.u. were converted to eV by using $R=13.60383$ eV and $I_\infty=79.003$ eV.

	Ref.	E_2	E_3	E_4	E_5	Γ_2	Γ_3	Γ_4	Γ_5	q_2	q_3	q_4	q_5
		(eV)				(meV)							
$2,0_n$													
Experiment	This work	60.147	63.658	64.467	64.816	37	10	4.0(5)	2.0(3)	−2.75	−2.5	−2.4	−2.4
	[1]	60.123(15)	63.652(7)	64.462(7)	64.813(7)	38(4)	8 (4)			−2.80(25)	−2(1)		
	[3]	60.151(10)				38(2)	8.3(20)			−2.6(3)	−2.5(5)		
	[4]	60.133(15)				38(1)				−2.75(5)			
Theory	This work	60.144	63.656	64.464	64.814	37.4	8.2	3.5	1.8	−2.77	−2.58	−2.55	−2.54
	[42]	60.172	63.664	64.467	64.816	37.4	8.5	3.6	1.9				
	[43]	60.190	63.667	64.467	64.813	40.2	8.9	3.9	1.2				
	[44]	60.151	63.656	64.462	64.812	38.3	8.4	3.6	1.9	−2.83	−2.67		
	[45]	60.152	63.659	64.464									
	[46]	60.155	63.658	64.465	64.815	36.2	8.4	3.4	1.8				
	[47]	60.155	63.662	64.469		36.6	8.4	3.6					
	[48]	60.147	63.656			37.8							
	[50]	60.175	63.664			39.9	8.8						
	[51]	60.154	63.656	64.463		36.5	7.9	3.3					
	[53]	60.145	63.656	64.465	64.814	37.4	8.2	3.5	1.8				
$2,1_n$													
Experiment	This work		62.758	64.135	64.657		0.5(3)	0.3(2)	<0.1		−3.5	−3.2	−3.2
	[1]		62.756(10)	64.139(17)	64.664(17)								
Theory	This work		62.758	64.134	64.656		0.105	0.055	0.027		−4.25	−3.32	−3.31
	[12]		62.761	64.138	64.660		0.104	0.054	0.027				
	[14]		62.758	64.136	64.657		0.116	0.052					
	[42]		62.752	64.144	64.662		0.143	0.021	0.013				
	[43]		62.764	64.107	64.627		0.12	0.052	0.055				
	[44]		62.755	64.132	64.654		0.112	0.057	0.028		−3.75	−2.93	−2.89
	[45]		62.760	64.135	64.655								
	[46]		62.758	64.135	64.657		0.106	0.056	0.028				
	[47]		62.759	64.135			0.095	0.060					
	[51]		62.756	64.132			0.098	0.047					
	[53]		62.758	64.134	64.657		0.105	0.056					
$2,-1_n$													
Experiment	This work		64.119	64.648	64.907		<0.05						
Theory	This work		64.118	64.648	64.906		0.0003	0.000004	$<10^{-6}$		−23	−132	197
	[12]		64.122	64.651			0.003	0.00097					
	[14]		64.119	64.647	64.907		0.0044						
	[42]		64.120	64.650	64.913		0.0303	0.0103					
	[44]		64.116	64.646	64.908		0.0016	0.0004	0.00003		−10.5	−15	−23
	[45]		64.118	64.651	64.909								
	[47]		64.124	64.650			0.00004	0.001					
	[51]		64.117	64.646			0.00053	0.00023					
	[53]		64.118	64.648	64.906		0.00044						

"+" states provides a quantitative estimate of the monochromator resolution, resulting in $n_m=20$ for $\Delta E\cong 4$ meV (FWHM).

With a suitable energy scale, high spectral resolution, and good signal-to-noise ratio, the first four members of the third "hidden" $2,-1_n(2p,nd)$ Rydberg series ($A=0$) were recently resolved [10]. As shown in Fig. 3, the nth state in the $2,-1_n$ series is very close to the $(n+1)$th state of the "−" series. Peak heights and linewidths of the resonance lines decrease by approximately two orders of magnitude when going from the "+" to the "−" series and further from the "−" to the $2,-1_n$ series. The latter resonances in particular

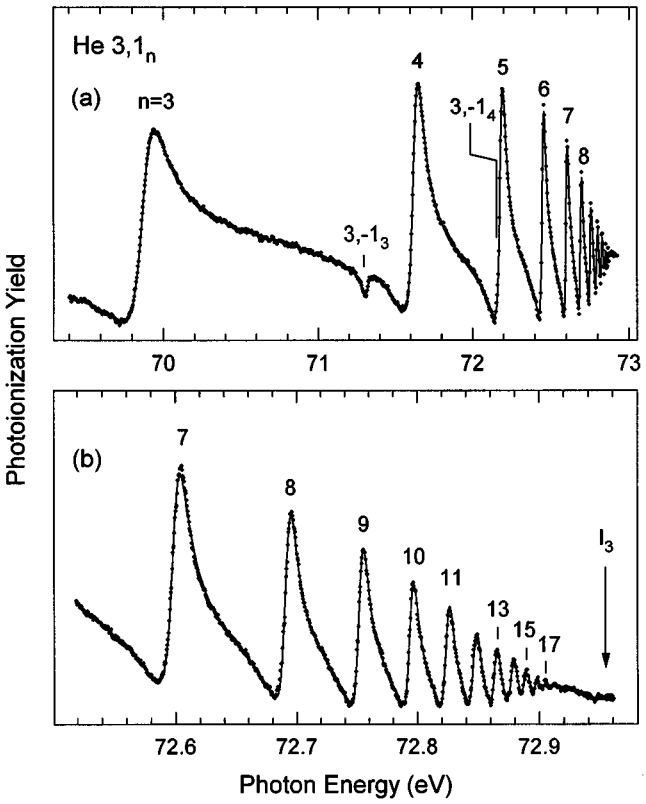

FIG. 4. Autoionizing resonances of doubly excited He below the $N=3$ threshold (I_3) of He: The principal series is $3,1_n$, and two resonances of the secondary series, $3,-1_n$, can be identified. The upper spectrum (a) gives an overview, while in the lower spectrum (b) the $n \geqslant 7$ region is displayed on an energy scale expanded by a factor of $\cong 8$.

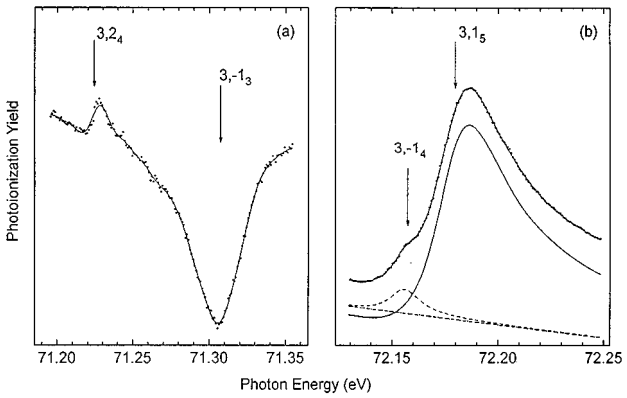

FIG. 5. Detailed study of the $3,-1_3$ and $3,1_5$ resonance regions of doubly excited He: (a) The first resonance, $3,2_4$, of a further secondary series below I_3 is clearly identified close to the $3,-1_3$ state. (b) The second resonance, $3,-1_4$, of the most intense secondary series, $3,-1_n$, shows up in the leading-edge region of the $3,1_5$ resonance.

are extremely long lived, and despite the neighboring $2,1_{n+1}$ and $2,-1_n$ lines observed in experiment, the *deconvoluted* resonances are separated from each other, justifying least-squares fits with independent Fano profiles. The fact that the linewidth of the $2,-1_3$ resonance is much narrower than the monochromator function renders this resonance ideally suited for determining the resolution of the monochromator. Here, we obtain $\Delta E=4$ meV (FWHM).

The reduced linewidth of the $N=2$ series, derived by least-squares fits, is $\Gamma^* \cong 200$ meV for the "+" series, $2,0_n$, $\Gamma^* \cong 8$ meV for the "−" series, $2,1_n$, and $\Gamma^* < 0.5$ meV for the $(2p,nd)$ series, $2,-1_n$, respectively, in fairly good agreement with the present theoretical results (see Table I). Both the experimental and the calculated Fano parameters of the separate resonances ($n=2$–5) are given in Table III and compared with previous experimental as well as selected theoretical results. The $N=2$ Rydberg series of the double excitations in He has been calculated most often, and a complete representation of *all* theoretical results would contain more than 30 references. There is obviously good agreement between the experimental and the theoretical results. Note the highly improved accuracy of the present experimental values as compared to previous results [1,3,4]. We note that for the most intense resonance, $2,0_2$ or $(sp,22+)$, a smaller linewidth is now obtained than previously found [9]: We now derive a Γ value of 37 ± 1 meV (instead of 42.3 meV before) and a q value of -2.75 ± 0.01 (instead of -2.55 before) for the $2,0_2$ resonance; the reason for this improvement is a rather low He pressure of 0.01 mbar, i.e., the almost complete absence of saturation effects. This improved Γ value is in much closer agreement with previous work (see Table III). Obvious saturation effects in the photoionization spectrum of Ref. [9], taken at a He pressure of 0.1 mbar, were most probably restricted to the $2,0_2$ line, however. In summary, all three $^1P^o$ Rydberg series predicted by theory below I_2 have now been resolved in our photoionization work. The $T=1$, $A=$"+" series, $2,0_n$, is the principal series, but also the two subsidiary series with correlation quantum numbers $T=0$ and $A=$"−" ($A=$"0") were observed.

C. Resonances below the $N=3$ and $N=4$ thresholds

For $N=3$ and $N=4$, five and seven $^1P^o$ series, respectively, are optically allowed from the ground state of He. Since the reduced transition probabilities, P^*, of the higher series with $T=0$ are predicted to be rather small (see Table I), we expect to identify, however, only 2 to 3 series in each case.

In Fig. 4, the photoionization spectrum for the energy region from 69.4 to $\cong 73$ eV is shown, containing Rydberg series below the $N=3$ threshold, I_3. The principal series, $3,1_n$, has been resolved now up to $n=17$; previously, with the 1221-line/mm grating, only states up to $n=13$ could be resolved [9]. The principal series can be well described by $\Gamma^*=3.1$ eV, a quantum defect of $\delta=0.815 \pm 0.002$, and a q value of $q=1.95 \pm 0.07$. The first member of a secondary Rydberg series at $\cong 71.3$ eV is also clearly visible; it is assigned to the first "bending vibrational" state with $K=N-4$. In addition, the first resonance of the most intense $T=0$ Rydberg series, $3,2_n$, can be seen: this $3,2_4$ state is expected to be $\cong 75$ meV below the $3,-1_3$ resonance, and in fact there is a weak feature at this very energy [see Fig. 5(a)]. However, due to its weakness, reliable results on linewidth and Fano-q parameter could not be obtained. We can estimate Γ to be smaller than the monochromator resolution and $|q|$ to be >1, both in agreement with the calculated values (see Table IV). The second member of the $3,-1_n$ series, $3,-1_4$, is ex-

TABLE IV. Comparison between experimental and theoretical values for resonance energies, E_n, linewidths (FWHM), Γ_n, and Fano-q parameters of the first members of the $N=3$ double-excitation Rydberg series of He. Unless otherwise stated, the error bars of the experimental values are ± 1 in the last digit. Conversion of literature values as in Table III.

	Ref.	E_3 (eV)	E_4	E_5	Γ_3 (meV)	Γ_4	Γ_5	q_3	q_4	q_5
$3,1_n$										
Experiment	This work	69.873(9)	71.623(4)	72.179(2)	181(10)	82(5)	39(3)	1.3(1)	1.8(1)	1.8(1)
	[1]	69.94(4)	71.66(1)	72.20(1)						
	[4]	69.914(15)			200(20)			1.32(5)		
	[5]	69.919(17)			132(26)			1.4(3)		
	[6]	69.917(12)	71.601(18)	72.181(15)	178(12)					
	[7]	69.88(2)	71.63(3)	72.17(3)	180(15)					
Theory	This work	69.871	71.624	72.180	191	78.8	35.4	1.25	1.64	1.53
	[29]	69.866	71.626	72.188						
	[30]	69.872	71.628	72.186						
	[52]	69.818	71.638	72.205						
	[54]	69.871	71.624	72.177	190	84.3	32.6			
	[58]	69.879	71.637	72.187	184	82	29			
	[59]	69.873	71.621	72.177	174	70.4	27.4	1.3	1.51	1.40
	[60]	69.875	71.622	72.177	189	88.2	34.0	1.26		
	[61]	69.871	71.624	72.180	190	78.8	35.3			
$3,-1_n$										
Experiment	This work	71.314(5)	72.160(3)		47(5)	23(10)		−0.1(1)	11(3)	
	[6]	71.30(4)			70					
	[7]	71.261(30)			73(15)					
Theory	This work	71.308	72.158	72.450	39.8	14.2	6.1	0.04	12.8	0.5
	[30]	71.316								
	[52]	71.411	72.213	72.481						
	[58]	71.320	72.171	72.458	37.4	18.2	6			
	[59]	71.309	72.156		35.5	14.0		−0.04	0.78	
	[60]	71.317	72.163	72.446						
	[61]	71.308	72.158		39.8	14.1				
$3,2_n$										
Experiment	This work		71.23(1)			<5			>1	
Theory	This work		71.223	71.999		0.93	0.60		3.3	4.5
	[52]		71.290	72.054						
	[56]		71.230	72.000		0.90	0.59			
	[58]		71.226	72.002		0.87	0.59			
	[59]		71.221	71.997		0.83	0.55		−17.9	−10.6
	[60]		71.219	71.992						
	[61]		71.223	71.999		0.90	0.59			

pected to be very close to this $3,1_5$ state; it can in fact be resolved on a magnified scale [see Fig. 5(b)]. The third member of this series, $3,-1_5$, however, cannot be separated experimentally from the $3,1_6$ state, since the two states are expected to differ in energy by only $\cong 3$ meV. Least-squares fits of the $3,-1_3$ and $3,-1_4$ resonances give linewidths of $\Gamma_3=47\pm5$ meV and $\Gamma_4=23\pm10$ meV, respectively, i.e., an almost constant reduced linewidth Γ^*. On the other hand, the q values of the resonances of the $3,-1_n$ series depend strongly on n: $q=-0.1$ for the $3,-1_3$ resonance, while it is 11 ± 3 for the $3,-1_4$ resonance. This is again in accord with the results of the complex-rotation-method calculations, which predict q values of 0.04 and 12.8 for the $3,-1_3$ and $3,-1_4$ resonances, respectively. This strong anomaly is probably due to an interaction between the $3,1_5$ and the $3,-1_4$ states, which represents an interaction between series with different symmetries, $v=(N-K-T-1)/2$: while the ''vibrational'' quantum number is $v=0$ for the $3,-1_n$ series, it is $=1$ for $3,-1_n$. This is obviously different from the ''usual'' strong interseries interferences, where only states from series with equal symmetries interact [11] (see below). We argue that the $3,1_5/3,-1_4$ interaction is favored by the small energy difference between the neighboring resonances, which is smaller than the linewidth of the $3,1_5$ resonance.

In Table IV, the results of both the present experimental work and the complex-rotation-method calculations are given for the low-n resonances of the $N=3$ series, in comparison to previous experimental and selected theoretical re-

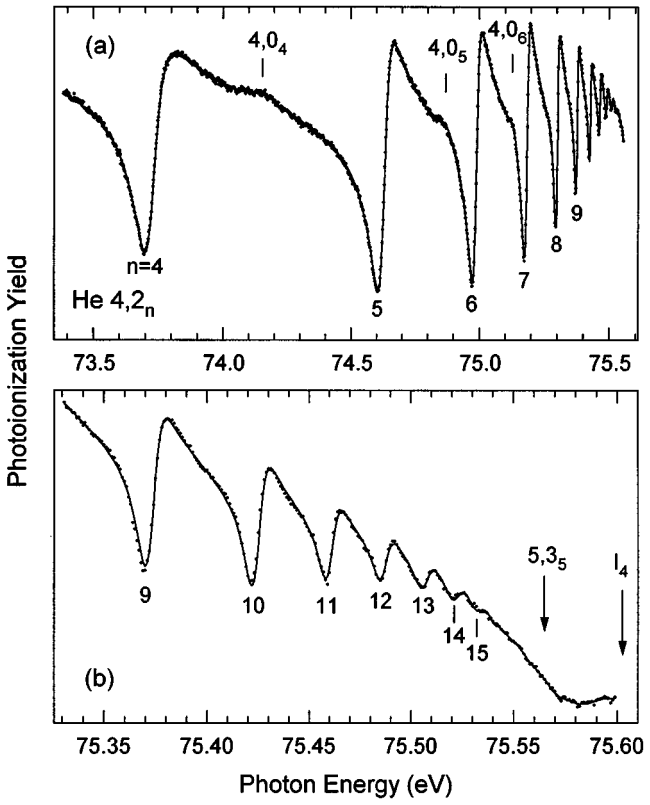

FIG. 6. Autoionizing resonances of doubly excited He below the $N=4$ threshold (I_4) of He: (a) overview, (b) the $n \geq 9$ region on an energy scale expanded by a factor of $\cong 8$. The principal series, $4,2_n$, and the first 3 resonances of the most intense secondary series, $4,0_n$, have been resolved. Note that the first member of the $N=5$ series, $5,3_5$, is situated close to, but slightly below, I_4.

sults. The experimental energies are less precise than in case of the $N=2$ series, due to the larger linewidths. Except for the results of Ref. [52], there is a very good agreement between all the experimental and theoretical values.

Figure 6 displays resonances below the $N=4$ threshold, I_4. Two series can be resolved in this spectrum, the principal $4,2_n$ series up to $n=15$, and the secondary $4,0_n$ series up to $n=6$. Contrary to the $N=2$ and $N=3$ cases, the secondary $4,0_n$ series shows a broader reduced linewidth ($\Gamma^* \cong 7$ eV) than the principal $4,2_n$ series ($\Gamma^*=3.2$ eV). This is due to the fact that additional decay channels, both with $K=2$ and $K=-2$, exist for the $K=0$ series, which overcompensate the normally expected decrease in linewidth for smaller K and T values. Moreover, the principal $4,2_n$ series is characterized by ''window'' resonances with $0<q<1$, whereas the $4,0_2$ series consists of ''positive'' resonances ($q>1$). The fit results in $q \cong 0.70$ (2.5) for the $4,2_n$ ($4,0_n$) series, in qualitative agreement with the calculations, which give $q \cong 0.48$ and $q \cong 3$ for $4,2_n$ and $4,0_n$, respectively. The high-n resonances of the $4,2_n$ series are superimposed on a ''background'', which is formed by the first resonance of the next series, $5,3_n$, at an energy close to I_4. The beginning of this interseries interference leads presumably to a quenching of the high-n members of the $4,2_n$ series. Results for the low-n resonances of the $N=4$ series are summarized in Table V, both from the present experiments and the complex-rotation-method calculations; they are compared with previous experimental and more recent theoretical results. The agreement between all the experimental and theoretical values is quite good again (except for those of Ref. [52]).

Different from the $N=3$ case, the third $N=4$ series ($4,-2_n$) cannot be resolved in the spectrum, although the reduced transition probabilities of the $3,2_n$ and $4,-2_n$ series are of similar magnitude. This is obviously due to the energies of the resonances: From calculations, the $4,-2_4$ resonance is expected to be between the $4,2_6$ and the $4,0_5$ resonances, i.e., on the leading edge of the $4,2_6$ resonance (see Table V and Fig. 6).

D. Interseries interferences for resonances below the $N=5$ and $N=6$ thresholds

In Fig. 7, double-excitation resonances below the $N=5$ threshold, I_5, and the $N=6$ threshold, I_6, are shown. Again, two series are clearly recognized, the principal $5,3_n$ ($6,4_n$) series and the weaker resonance lines of the $5,1_n$ ($6,2_n$) secondary series. The reduced linewidths of the $5,1_n$ ($6,2_n$) lines are again broader than those of the principal $5,3_n$ ($6,4_n$) series. All these series consist of ''window'' resonances. A strong perturbation of the high-n Rydberg resonances of the $5,3_n$ series by the first member of the next series, ($6,4_6$), is clearly visible in the spectrum. A similar perturbation of the $6,4_n$ resonance by $7,5_7$ is also present. In both cases, anomalous intensities, linewidths, and energies of the resonance lines can be easily recognized. Such anomalies were first observed in double-excitation spectra of He taken about four years ago [9], but have recently been investigated in more detail [11]. We first notice that within the interference, the reduced linewidth as a function of quantum number n follows a Fano-like profile, with the $n=9$ resonance being narrower, and the $n=11$ and $n=12$ resonances much broader than the linewidths expected on the basis of a constant reduced linewidth of the unperturbed Rydberg series. Furthermore, the envelope of the $5,3_n$ ($6,4_n$) resonances does *not* represent the $6,4_6$ ($7,5_7$) resonance; instead, the $6,4_6$ ($7,5_7$) line is expected to be at the center of the Fano profile close to the $5,3_{10}$ ($6,4_{10}$) resonance (see Fig. 7).

For the low-n members of the $N=5$ and $N=6$ principal series (below the interference region), the experimental and theoretical values are again tabulated in Table VI in comparison to the relatively few available previous results. The results of the present complex-rotation-method calculations for the interference region are compared with the experimental results in a graphical form. The bar diagrams in Fig. 7 represent the calculated energies of the resonances, both of the principal and the most intense secondary series. The lengths of the vertical bars represent the calculated linewidths in case of the principal series, $5,3_n$ and $6,4_n$; the absolute scale is given by the 50-meV length in Fig. 7(b). Similar to the case of an undisturbed series, the peak heights are roughly related to the theoretical linewidths, an observation that is again caused by convolution with the monochromator function. Previous calculations for the interference region were solely based on the hyperspherical close-coupling method [13,15], with the most recent one [15] being in excellent agreement with the results of the present complex-rotation-method calculations (see Table II).

An interference similar to that of the $5,3_n/6,4_6$ ($6,4_n/7,5_7$) interaction of the principal series with $v=0$ symmetry is also expected to occur between secondary series, e.g., those with $v=1$ symmetry $5,1_n/6,2_n$. However, these interferences cannot be seen in the experiment, due to the overlap of the strong $5,3_n$ ($6,4_n$) with the weaker $5,1_n$ ($6,2_n$) series, particularly in the case of higher n numbers. In our spectra there is no hint that series with different symmetry, as, e.g., the $v=0$ and $v=1$ series, interfere, in agreement with theoretical predictions [64].

The transition probabilities are quite low for all Rydberg series with $N\geqslant 5$, which means that high He pressures of $\geqslant 1$ mbar were needed to obtain good statistics. Under these conditions (high pressure, high background), saturation effects may occur, which are difficult to isolate in the experiment. Such saturation effects influence only slightly the measured linewidths, since all Γ values are very close to or even smaller than the monochromator resolution. The effects on the q parameters, however, will be much stronger, with additional complications arising from the high density of resonances leading to an overlap of resonance wings. This means that the derived q values are trustworthy only in a qualitative sense. There is no doubt that *all* measured resonances in the Rydberg series with $N>5$ are window resonances ($|q|<1$). In this way, we find a change in q from $\cong -0.3$ for $5,3_5$ to values close to zero in the interference region. The question of a q reversal, as sometimes predicted by theory (see Table II), cannot be decided on the basis of the present experiments. It should be noted that this question will probably remain open even if spectra with better resolution and better statistical accuracy should become available, since there is a strong overlap of broad resonances of the principal $5,3_n$ and the secondary $5,1_n$ series, preventing their experimental separation. Especially for the $5,3_{10}$ and $6,4_{10}$ resonances, the overlaps with the $5,1_9$ and $6,2_9$ resonances, respectively, are very strong, and the measured peak heights and linewidths surpass the calculated values. It should be mentioned that also the calculated Fano-q values become increasingly more doubtful for high N numbers ($N\geqslant 6$), and that both experiment and theory do not yield reliable Fano-q parameters in this double-excitation region.

E. Interseries interferences below the $N=7$ and $N=8$ thresholds

In Fig. 8, double-excitation resonances below the $N=7$, $N=8$, and $N=9$ ionization thresholds of He are shown, with experimental and theoretical results compared again in a graphical way. We are not aware of any other experimental and theoretical results for this energy region. Here, the signal-to-background ratio is less than 0.001, and a reliable fit of the $N=9$ series cannot be performed: for $h\nu>78.08$ eV, the solid line through the data points is just a guide to the eyes. Two interference regions occur in these spectra for each principal N series, e.g., the $8,6_8$ and $8,6_9$ resonances interfere with the $7,5_n$ series in the $n=10$–14 and $n=15$–18 regions, respectively. Moreover, the intensity modulations and linewidth variations are much stronger than for the $N=5$ and $N=6$ series. This supports the Fano-like variation of the reduced linewidths as a function of n: here, the most ''destructive'' interference occurs for *integer n* values, whereas it is *between* two integer n values in case of the $N=5$ and $N=6$ series. Note that the $7,5_{10}$ and $7,5_{15}$ ($8,6_{11}$ and $8,6_{15}$) reso-

TABLE V. Comparison between experimental and theoretical values for resonance energies, E_n, linewidths (FWHM), Γ_n, and Fano-q parameters of the first members of the $N=4$ double-excitation Rydberg series of He. Unless otherwise stated, the error bars of the experimental values are ± 1 in the last digit. Conversion of literature values as in Table III.

	Ref.	E_4	E_5 (eV)	E_6	Γ_4	Γ_5 (meV)	Γ_6	q_4	q_5	q_6
$4,2_n$										
Experiment	This work	73.715(6)	74.620(4)	74.979(2)	94	59	32	0.5	0.7	0.7
	[1]	73.758(22)	74.642(23)	74.999(23)						
	[6]	73.66(3)	74.57(3)	74.93(3)						
	[7]	73.72(3)	74.60(3)	74.96(3)	89(8)					
Theory	This work	73.711	74.616	74.975	97.3	59.0	32.8	0.29	0.47	0.49
	[30]	73.702	74.633	74.992						
	[52]	73.680	74.601	74.997						
	[54]	73.710	74.615	74.906	98	61	19			
	[63]	73.705	74.636	74.994						
$4,0_n$										
Experiment	This work	74.13	74.89	75.12	100(10)	66(10)	35(10)	3	3	>3
	[7]	74.13(3)	74.77(3)							
Theory	This work	74.138	74.848	75.122	130	62	38	2.5	2.3	3.9
	[30]	74.213								
	[52]	74.259	74.954	75.178						
	[54]	74.138	74.847		129	56				
	[63]	74.214	74.901	75.148						
$4,-2_n$										
Theory	This work	74.907	75.160	75.289	21	6.4	3.6			
	[52]	74.960	75.190							

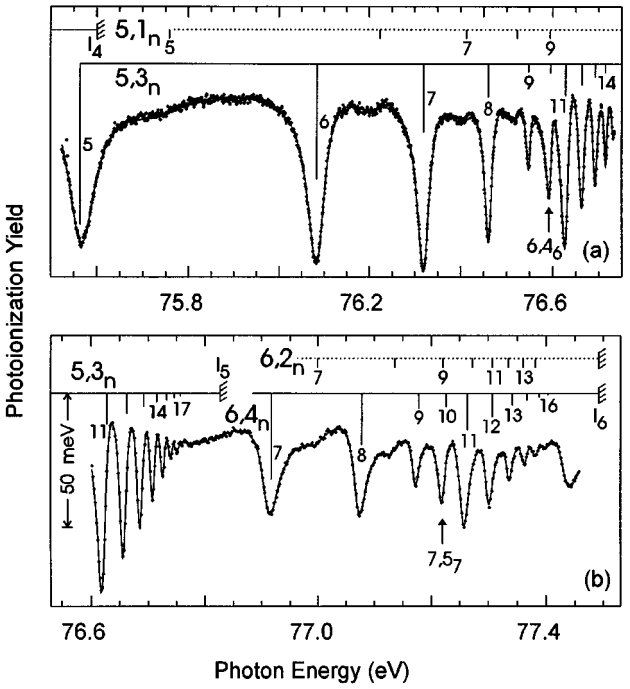

FIG. 7. Double-excitation resonances of He below the (a) $N=5$ and (b) $N=6$ thresholds of He in comparison to the calculated energies (vertical bar diagrams) as well as to the calculated linewidths ($5,3_n$ and $6,4_n$ series). The calculated positions of the perturber states are marked by vertical arrows. For the principal series, the lengths of the vertical bars are proportional to the theoretical linewidths. For the secondary series, the dotted bar diagrams represent only the theoretical energies of the resonances.

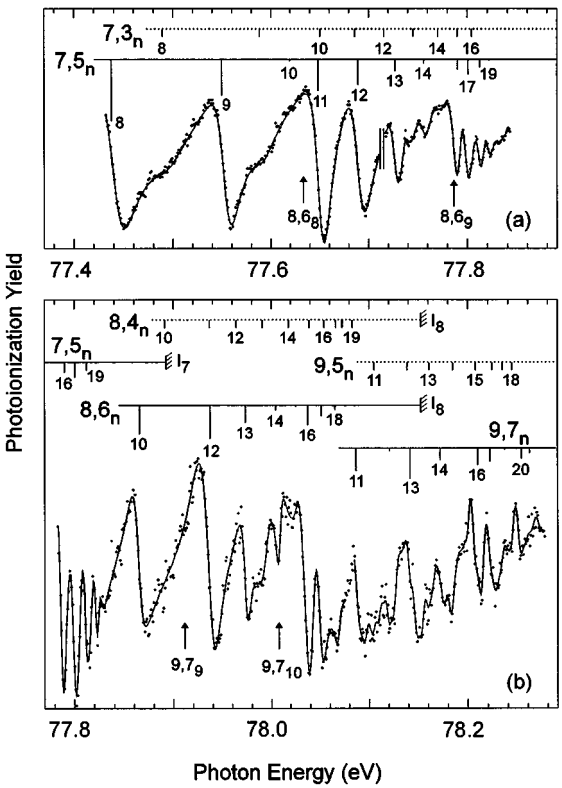

FIG. 8. Double-excitation resonances of He below the (a) $N=7$, (b) $N=8$, and $N=9$ thresholds of He. The vertical bar diagrams and vertical arrows have the same meaning as in Fig. 7. Note that a least-squares fit of independent Fano profiles has been performed only in the region below 78.07 eV; beyond this energy, the solid curve through the data points serves just as a guide to the eyes.

nances are almost completely suppressed.

Again, the $v=1$ series with $K=N-4$ are resolved as well. These resonances, however, overlap strongly with the principal ($v=0$) series, and are visible only as shoulders of the principal resonances: At least the $7,3_8$, $7,3_9$, $7,3_{13}$, $7,3_{14}$, $8,4_{10}$, and $8,4_{13}$ resonances can be clearly identified. As in case of the $N=5$ and $N=6$ series, an overlap between principal and secondary series occurs in this energy region.

TABLE VI. Comparison between experimental and theoretical values for resonance energies, E_n, and linewidths (FWHM), Γ_n, of the first members of the $N=5$ and $N=6$ double-excitation Rydberg series of He below the interseries interferences. Conversion of literature values as in Table III.

	Ref.	E_5	E_6	E_7	E_8	Γ_5	Γ_6	Γ_7	Γ_8
		(eV)				(meV)			
$5,3_n$									
Experiment	This work	75.566(5)	76.083(3)	76.320(2)	76.461(1)	65(2)	39.5(8)	25.2(8)	14.2(8)
	[6]	75.54(4)	76.10(3)	76.30(3)					
	[7]	75.58(3)	76.13(3)	76.31(3)					
Theory	This work	75.564	76.084	76.320	76.461	59.3	42.5	25.2	12.4
	[15]	75.564	76.081	76.319	76.459	61.5	41.1	25.2	12.7
	[19]	75.55	76.10						
	[54]	75.563	76.084			59.9	40.8		
$6,4_n$									
Experiment	This work		Perturber	76.918(2)	77.078(1)			34.9(1.5)	20.4(6)
	[7]		76.61(3)	76.89(3)			27(10)		
Theory	This work		76.592	76.918	77.078		40.6	32.3	19.5
	[15]		76.592	76.918	77.077		40.5	31.3	19.6
	[54]		76.592				39.4		

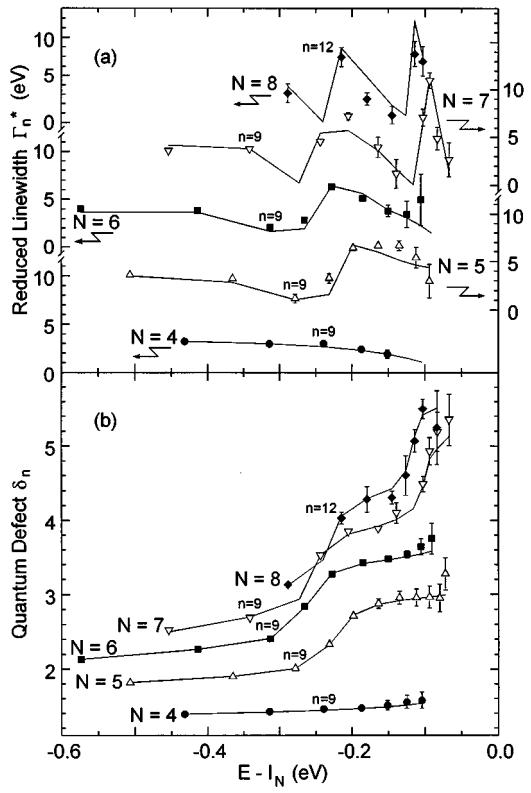

FIG. 9. Graphical representation of experimental and theoretical results for the principal series $N=4$ to $N=8$: (a) reduced linewidth, $\Gamma_n^*=\Gamma_n n^{*3}$; (b) quantum defect, δ_n. Both are plotted as a function of the term energy, i.e. the energy difference to the relevant ionization threshold, I_N. The experimental results are given by the various symbols $N=4$ (●), $N=5$ (△), $N=6$ (■), $N=7$ (▽), and $N=8$ (◆); the solid lines connect the theoretical results for different n. For clarity, the ordinate in (a) is shifted by 6.5 eV between neighboring N series.

VI. COMPARISON BETWEEN EXPERIMENT AND THEORY

The experimental and theoretical results of the present work for the Fano parameters (energy, linewidth, q value) of the first resonances of the noninterfering $N=2$, 3, and 4 double-excitation Rydberg series are summarized in Tables III to V. The comparison shows an excellent agreement between theory and experiment. This holds as well for the high-n members of these series. There are constant Γ^*, q, and δ values for each series, except for resonances with low quantum numbers n, which are influenced by the inner electron, N. This effect is borne out both in experiment and in theory (see Tables III to VI).

For the interfering series with $N\geqslant 5$, a comparison between theory and experiment has been given in the form of a table only for the low-n resonances; in the interference regions, such a comparison has been given instead in Figs. 7, 8, and 9 in a graphical way. The vertical bars in Figs. 7 and 8 represent the calculated energies (positions of the bars) and the calculated linewidths (lengths of the bars) for the principal series $5,3_n$, $6,4_n$, $7,5_n$, $8,6_n$, and $9,7_n$; for the secondary series $N,(N-4)_n$, the bars represent only the resonance energies. There is obviously close agreement between theory and experiment for both the energies and the peak heights; the latter are roughly proportional to the linewidths.

For a closer insight into the behavior of the resonances, we show in Fig. 9(a) the reduced linewidths, Γ_n^*, and in Fig. 9(b) the quantum defects, δ_n, for the $N=4$ to $N=8$ principal series as a function of the term energy $E(n,N)-I_N$. The symbols represent fitted experimental results for the measured resonances; the solid lines connect the *theoretical* Γ_n^* and δ_n values for different N. The two results agree very well, and the small deviations visible can be explained by overlapping principal and secondary series in the experimental spectrum. The reduced linewidths show destructive and constructive interferences in the energy regions of the interseries interferences (''Fano-like profile''). The quantum defects exhibit increases by one in the interseries interference regions, and the positions and linewidths of these increases represent the energies and linewidths of the perturber state [68]. In case of the $N=7$ and $N=8$ series, the *two* interseries interferences are reflected in two Fano-like profiles in Γ_n^* and in two increases of δ_n by one. It is interesting to analyze also the Γ_n^* and δ_n structure of the $N=4$ series: both Γ_n^* and δ_n behave as expected for a *beginning* interseries interference, whose realization is hindered due to unresolved high-n features.

VII. SUMMARY AND PERSPECTIVES

In the present work we reported on the observation of 18 different Rydberg series in the $^1P^o$ double-excitation resonance region of He. This includes the complete set of the three dipole-allowed $N=2$ Rydberg series, three series among the five optically allowed $N=3$ Rydberg series, and two series each for $N=4$, 5, 6, 7, 8, and 9. Energies, linewidths, and—if applicable—Fano-q parameters were derived for the various resonances from the experimental data; they agree very well with the results of complex-rotation-method calculations for the $N=2$, $N=3$, and $N=4$ series. For the higher series, good agreement between experiment and theory was found for energies and linewidths, but only qualitative agreement for the Fano-q parameter (''window resonances''). For $N\geqslant 5$, strong interseries interferences were both theoretically predicted and experimentally observed, resulting in Fano-like variations of the reduced linewidths and increases in the quantum defects by one across the interference regions.

Upon submittal of this manuscript, a remarkable improvement in resolution to $\Delta E=1$ meV (FWHM) has been achieved by a group of researchers led by two of the present authors using the high-resolution beamline 9.0.1 at the Advanced Light Source (ALS) in Berkeley [69]. Since other workers had shortly before reached at the same beamline a resolution of just $\Delta E\cong 6.5$ meV (FWHM) [70], further rapid progress in resolving power in this spectral region can be expected. In combination with the high photon flux available at third-generation undulator beamlines, such high spectral resolution will offer new opportunities in the study of long-lived atomic and molecular states.

ACKNOWLEDGMENTS

This work was supported by the Bundesminister für Bildung, Wissenschaft, Forschung und Technologie, Project No. 05-650 KEA. Technical help by the staff of BESSY is highly appreciated, in particular the efforts in improving the small-source optics of the electron storage ring. The authors appreciate highly beneficial discussions with D. A. Shirley in the early stages of this work.

[1] R. P. Madden and K. Codling, Phys. Rev. Lett. **10**, 516 (1963); Astrophys. J. **141**, 364 (1965).
[2] J. W. Cooper, U. Fano, and F. Prats, Phys. Rev. Lett. **10**, 518 (1963).
[3] H. D. Morgan and D. L. Ederer, Phys. Rev. A **29**, 1901 (1984).
[4] H. Kossmann, B. Krässig, and V. Schmidt, J. Phys. B **21**, 1489 (1988).
[5] P. Dhez and D. L. Ederer, J. Phys. B **6**, L59 (1973).
[6] P. R. Woodruff and J. A. R. Samson, Phys. Rev. A **25**, 848 (1982).
[7] M. Zubek, G. C. King, P. M. Rutter, and F. H. Read, J. Phys. B **22**, 3411 (1989).
[8] M. Domke, T. Mandel, A. Puschmann, C. Xue, D. A. Shirley, G. Kaindl, H. Petersen, and P. Kuske, Rev. Sci. Instrum. **63**, 80 (1992).
[9] M. Domke, C. Xue, A. Puschmann, T. Mandel, E. Hudson, D. A. Shirley, G. Kaindl, C. H. Greene, H. R. Sadeghpour, and H. Petersen, Phys. Rev. Lett. **66**, 1306 (1991).
[10] M. Domke, G. Remmers, and G. Kaindl, Phys. Rev. Lett. **69**, 1171 (1992).
[11] M. Domke, K. Schulz, G. Remmers, A. Gutiérrez, G. Kaindl, and D. Wintgen, Phys. Rev. A **51**, R4309 (1995).
[12] T. N. Chang, Phys. Rev. A **47**, 3441 (1993).
[13] J.-Z. Tang, S. Watanabe, M. Matsuzawa, and C. D. Lin, Phys. Rev. Lett. **69**, 1633 (1992).
[14] J.-Z. Tang, S. Watanabe, and M. Matsuzawa, Phys. Rev. A **48**, 841 (1993).
[15] J.-Z. Tang and I. Shimamura, Phys. Rev. A **50**, 1321 (1994).
[16] D. Wintgen and D. Delande, J. Phys. B **26**, L399 (1993).
[17] R. N. S. Sodhi and C. E. Brion, J. Electron Spectrosc. Relat. Phenom. **34**, 363 (1984).
[18] J. M. Rost and J. S. Briggs, J. Phys. B **24**, 4293 (1991).
[19] D. R. Herrick and O. Sinanoglu, Phys. Rev. A **11**, 97 (1975).
[20] C. D. Lin, Phys. Rev. A **29**, 1019 (1984); Adv. At. Mol. Phys. **22**, 77 (1986).
[21] H. R. Sadeghpour and C. H. Greene, Phys. Rev. Lett. **65**, 313 (1990).
[22] U. Fano, Phys. Rev. **124**, 1866 (1961).
[23] U. Fano and J. W. Cooper, Phys. Rev. **137**, A1364 (1965).
[24] P. G. Burke and D. D. McVicar, Proc. Phys. Soc. London **86**, 989 (1965).
[25] P. G. Burke and A. J. Taylor, Proc. Phys. Soc. London **88**, 549 (1966).
[26] P. L. Altick and E. N. Moore, Proc. Phys. Soc. London **92**, 853 (1967); Phys. Rev. **147**, 59 (1966).
[27] G. W. F. Drake and A. Delgarno, Proc. R. Soc. London A **320**, 549 (1971).
[28] A. K. Bhatia and A. Temkin, Phys. Rev. A **29**, 1895 (1984).
[29] K. T. Chung, Phys. Rev. A **6**, 1809 (1972).
[30] R. S. Oberoi, J. Phys. B **5**, 1120 (1972).
[31] P. G. Burke and A. J. Taylor, J. Phys. B **2**, 44 (1969).
[32] S. Ormonde, W. Whitaker, and L. Lipsky, Phys. Rev. Lett. **19**, 1161 (1967).
[33] V. S. Senashenko and A. Wague, J. Phys. B **12**, L269 (1979).
[34] Y. K. Ho, J. Phys. B **12**, 387 (1979).
[35] Y. K. Ho, Phys. Lett. **79A**, 44 (1980).
[36] L. Lipsky and M. J. Conneely, Phys. Rev. A **14**, 2193 (1976).
[37] M. J. Conneely and L. Lipsky, J. Phys. B **11**, 4135 (1978).
[38] K. T. Chung and I. Chen, Phys. Rev. Lett. **28**, 783 (1972).
[39] Y. K. Ho, Phys. Rev. A **23**, 2137 (1981).
[40] K. A. Berrington, P. G. Burke, W. C. Fon, and K. T. Taylor, J. Phys. B **15**, L603 (1980).
[41] Y. Komninos and C. A. Nicolaides, Phys. Rev. A **34**, 1995 (1986).
[42] A. Macias, T. Martin, A. Riera, and M. Yunez, Phys. Rev. A **36**, 4187 (1987).
[43] P. Hamacher and J. Hinze, J. Phys. B **22**, 3397 (1989).
[44] I. Sanchez and F. Martin, J. Phys. B **23**, 4263 (1990).
[45] A. G. Abrashkevich, D. G. Abrashkevich, M. S. Kachiev, I. V. Puzynin, and S. I. Vinitsky, Phys. Rev. A **45**, 5274 (1992).
[46] D. H. Oza, Phys. Rev. A **33**, 824 (1986).
[47] L. Wu and J. Xi, J. Phys. B **23**, 727 (1990).
[48] T. N. Chang, Phys. Rev. A **47**, 705 (1993).
[49] C. Froese-Fischer and M. Idrees, J. Phys. B **23**, 679 (1990).
[50] T. Brage, C. Froese-Fischer, and G. Miecznik, J. Phys. B **25**, 5289 (1992).
[51] R. Moccia and P. Spizzo, J. Phys. B **20**, 1423 (1987).
[52] H. Fukuda, N. Koyama, and M. Matsuzawa, J. Phys. B **20**, 2959 (1987).
[53] Y. K. Ho, Z. Phys. D **21**, 191 (1991).
[54] Y. K. Ho, J. Phys. B **15**, L691 (1982).
[55] M. A. Hayes and M. P. Scott, J. Phys. B **21**, 1499 (1988).
[56] S. Salomonson, S. L. Carter, and H. P. Kelly, Phys. Rev. A **39**, 5111 (1989).
[57] S. Salomonson, S. L. Carter, and H. P. Kelly, J. Phys. B **18**, L149 (1985).
[58] R. Moccia and P. Spizzo, Phys. Rev. A **43**, 2199 (1991).
[59] I. Sánchez and F. Martin, Phys. Rev. A **44**, 7318 (1991).
[60] B. Zhou and C. D. Lin, J. Phys. B **26**, 2575 (1993).
[61] Y. K. Ho, Phys. Rev. A **44**, 4154 (1991).
[62] F. Martin, Phys. Rev. A **48**, 331 (1993).
[63] O. Robaux, J. Phys. B **20**, 2347 (1987).
[64] A. Bürgers and D. Wintgen, J. Phys. B **27**, L131 (1994).
[65] W. P. Reinhardt, Annu. Rev. Phys. Chem. **33**, 223 (1982).
[66] Y. K. Ho, Phys. Rep. **99**, 1 (1983).
[67] D. Delande, A. Bommier, and J. C. Gay, Phys. Rev. Lett. **66**, 141 (1991).
[68] M. J. Seaton, Proc. Phys. Soc. **88**, 815 (1966).
[69] G. Kaindl, K. Schulz, P. A. Heimann, J. D. Bozek, and A. S. Schlachter, Synchr. Rad. News **8** (5), 29 (1995).
[70] C. D. Caldwell, A. Menzel, S. P. Frigo, S. B. Whitfield, and M. O. Krause, Synchr. Rad. News **8** (1), 23 (1995).